# Poly(rC)-binding protein 1 limits hepatitis C virus virion assembly and secretion

**Sophie E. Cousineau[1], Marylin Rheault[1], and Selena M. Sagan[1,2]#**

[1]Department of Microbiology & Immunology, McGill University, Montreal, QC, Canada

[2]Department of Biochemistry, McGill University, Montreal, QC, Canada

#Corresponding Author: Dr. Selena Sagan, McGill University, 3655 Promenade Sir William Osler, Room 805, Montréal, QC, H3G 1Y6; email: selena.sagan@mcgill.ca

**Keywords:** Hepatitis C virus (HCV), poly(rC)-binding protein 1 (PCBP1), hnRNP E1, assembly, virion secretion

**Running title**: PCBP1 limits HCV assembly and secretion

**ABSTRACT**

The hepatitis C virus (HCV) co-opts numerous cellular elements – including proteins, lipids, and microRNAs – to complete its viral life cycle. The cellular RNA-binding protein, poly(rC)-binding protein 1 (PCBP1), was previously reported to bind to the 5′ untranslated region (UTR) of the HCV genome; however, its importance in the viral life cycle has remained unclear. Herein, we sought to clarify the role of PCBP1 in the HCV life cycle. Using the HCV cell culture (HCVcc) system, we found that knockdown of endogenous PCBP1 resulted in an overall decrease in viral RNA accumulation, yet resulted in an increase in extracellular viral titers. To dissect PCBP1's specific role in the HCV life cycle, we carried out assays for viral entry, translation, genome stability, RNA replication, as well as virion assembly and secretion. We found that PCBP1 knockdown did not directly affect viral entry, translation, RNA stability, or RNA replication, but resulted in an overall increase in infectious particle secretion. This increase in virion secretion was evident even when viral RNA synthesis was inhibited, and blocking virus secretion could partially restore the viral RNA accumulation decreased by PCBP1 knockdown. We therefore propose a model where endogenous PCBP1 normally limits virion assembly and secretion, which increases viral RNA accumulation in infected cells by preventing the departure of viral genomes packaged into virions. Overall, our findings improve our understanding of how cellular RNA-binding proteins influence viral genomic RNA utilization during the HCV life cycle.

34 **INTRODUCTION**

35 Hepatitis C virus (HCV) is an enveloped virus of the *Flaviviridae* family (genus: hepacivirus)
36 that typically causes a persistent liver infection (1). Its ~9.6 kb single-stranded, positive-sense
37 RNA genome contains a single open reading frame flanked by 5′ and 3′ untranslated regions
38 (UTR). A highly structured internal ribosomal entry site (IRES) in the 5′ UTR drives the
39 translation of the viral polyprotein, which is subsequently processed into 10 mature viral
40 proteins: 3 structural proteins (core, E1 and E2 glycoproteins), and 7 non-structural (NS) proteins
41 (p7, NS2, NS3, NS4A, NS4B, NS5A and NS5B) (1, 2). While the structural proteins form the
42 nucleocapsid and viral envelope, the NS3-5B proteins form the viral replicase, required for viral
43 RNA replication (3). The p7, NS2, NS3 and NS5A proteins are also implicated in viral genome
44 packaging and the assembly of viral particles (4-7). As a positive-sense RNA virus, the HCV
45 genome itself must serve as a template for viral translation, genome replication, and packaging;
46 however, the mechanisms that determine which process each viral RNA is engaged in at any
47 given time have not been well defined. Importantly, due to their limited coding capacity, viruses
48 are highly dependent on the molecular machinery of the host cell. While numerous cellular
49 proteins and RNAs have been shown to interact with the HCV genome, their precise role(s) in
50 the viral life cycle often remain poorly defined.

51 The poly(rC)-binding protein 1 (PCBP1), along with its paralogs hnRNP K and PCBP2,
52 is one of the most abundant cellular RNA-binding proteins with an affinity for poly(rC) (8).
53 These multifunctional proteins can regulate translation and enhance the stability of their cellular
54 mRNA targets, which they interact with through their hnRNP K homologous (KH) domains (9).
55 Notably, all three paralogs have been reported to bind to the HCV 5′ UTR (10-12). However, the
56 degree to which each protein has been studied in the context of HCV infection varies

57 significantly – while hnRNP K and PCBP2 have been fairly extensively studied and reported to
58 play markedly different roles in the viral life cycle, the role of PCBP1 in the HCV life cycle has
59 not been investigated in detail (13, 14). Beyond its interactions with the 5′ UTR, previous reports
60 suggested that PCBP1 was not necessary for HCV IRES-mediated translation, but that
61 knockdown of PCBP1 decreases HCV RNA accumulation during infection (15, 16).
62 Herein, we sought to further clarify the role of PCBP1 in the HCV life cycle. Using cell
63 culture-adapted strains of HCV (HCVcc), we found that PCBP1 knockdown decreased viral
64 RNA accumulation, yet led to an increase in virion secretion. By examining individual steps of
65 the viral life cycle, we ruled out a direct role for PCBP1 in viral entry, translation, genome
66 stability and viral RNA replication. Further analysis of the assembly step revealed that, similarly
67 to its paralog hnRNP K, endogenous PCBP1 limits HCV virion assembly and release.
68
69 **MATERIALS AND METHODS**
70 **Cell culture**
71 Huh-7.5 human hepatoma cells were obtained from Charlie Rice (Rockefeller University) and
72 maintained in complete media: Dulbecco's Modified Eagle Media (DMEM) supplemented with
73 inactivated 10% fetal bovine serum (FBS), 2 mM L-glutamine, and 1X MEM non-essential
74 amino acids. Human embryonic kidney (293T) cells were kindly provided by Martin J. Richer
75 (McGill University, Montreal, QC, Canada) and were maintained in DMEM supplemented with
76 10% FBS. All cell lines were maintained at 37°C/5% $CO_2$ and were routinely screened for
77 mycoplasma contamination.
78

79 **Plasmids and viral RNAs**

80 The pJFH-$1_T$ plasmid, encoding a cell culture-adapted Japanese Fulminant Hepatitis (JFH-1;
81 HCV genotype 2a) with three adaptive mutations that increase viral titers in cell culture, was
82 provided by Rodney Russell (Memorial University of Newfoundland) (17). The pJ6/JFH1
83 plasmid bears a full-length viral sequence derived from the J6 (structural genes through first
84 transmembrane domain of NS2) and JFH-1 (remaining NS genes) isolates of HCV, and the
85 pJ6/JFH-1 FL RLuc GNN ("RLuc-GNN") viral sequence also includes a *Renilla* luciferase
86 (RLuc) reporter gene inserted between p7 and NS2 and an inactivating GNN mutation within the
87 NS5B RNA polymerase active site (4, 18). The pJ6/JFH-1 mono RLuc-NS2 plasmid ("Δcore-
88 p7") – a truncated version of the *Renilla* reporter virus with a deletion of the structural genes
89 through p7 – was provided by Joyce Wilson (University of Saskatchewan) (19).

90 To make full-length uncapped viral RNAs, all plasmid templates were linearized and *in*
91 *vitro* transcribed as previously described (20). The firefly luciferase (FLuc) mRNA was transcribed
92 from the Luciferase T7 Control DNA plasmid (Promega) linearized using *XmnI* and *in vitro*
93 transcribed using the mMessage mMachine T7 Kit (Life Technologies) according to the
94 manufacturer's instructions.

95

96 **Generation of infectious HCV stocks**

97 To generate JFH-$1_T$ stocks, 30 µg of *in vitro* transcribed RNA was transfected into Huh-7.5 cells
98 using the DMRIE-C reagent (Life Technologies) according to the manufacturer's instructions.
99 Four days post-transfection, infectious cell supernatants were passed through a 0.45 µm filter and
100 infectious viral titers were determined by focus-forming unit assay (17). Infectious virus was
101 amplified for two passages through Huh-7.5 cells at a MOI of 0.2 before being used for

102 infections. To generate J6/JFH-1 stocks, 25 µg of *in vitro* transcribed RNA was electroporated
103 into 6 x $10^6$ Huh-7.5 cells using a Bio-Rad GenePulser XCell at 270 V, 950 µF, and infinite
104 resistance in a 4-mm cuvette. Two days post-electroporation, infectious cell supernatants were
105 passed through a 0.45 µm filter and concentrated at least 10-fold using Amicon Ultra-15-100K
106 centrifugal filter units (Millipore Sigma) according to the manufacturer's instructions. Viral titers
107 were determined by focus-forming unit assay. All viral stocks were aliquoted and stored at -80°C
108 until use.
109
110 **Focus-forming unit (FFU) assays**
111 One day prior to infection, 8-well chamber slides (Lab-Tek) were seeded with 4 x $10^5$ Huh-7.5
112 cells/well. Infections were performed with 10-fold serial dilutions of viral samples in 100 µL for
113 4 h, after which the supernatant was replaced with fresh media. Three days post-infection, slides
114 were fixed in 100% acetone and stained with anti-HCV core antibody (1:100, clone B2,
115 Anogen), and subsequently with the AlexaFluor-488-conjugated anti-mouse antibody (1:200,
116 ThermoFisher Scientific) for immunofluorescence analysis. Viral titers are expressed as the
117 number of focus-forming units (FFU) per mL.
118 Extracellular virus titers were determined directly from cell supernatants, while
119 intracellular virus titers were determined after cell pellets were subjected to lysis via four freeze-
120 thaw cycles, removal of cellular debris via centrifugation, and recovery of virus-containing
121 supernatants.

122

123 **MicroRNAs and siRNA sequences**

124 siGL3 (siCTRL): 5'-CUUACGCUGAGUACUUCGAUU-3', siGL3* : 5'-

125 UCGAAGUACUCAGCGUAAGUU-3', miR122$_{p2-8}$ (siCTRL for luciferase experiments): 5'-

126 UAAUCACAGACAAUGGUGUUUGU-3', miR122$_{p2-8}$*: 5'-

127 AAACGCCAUUAUCUGUGAGGAUA-3' (21), siPCBP1: 5'-

128 CUGUGUAAUUUCUGGUCAGUU-3', siPCBP1*: 5'-CUGACCAGAAAUUACACAGUU-3'

129 (16) were all synthesized by Integrated DNA Technologies.

130 All microRNA and siRNA duplexes were diluted to a final concentration of 20 µM in

131 RNA annealing buffer (150 mM HEPES pH 7.4, 500 mM potassium acetate, 10 mM magnesium

132 acetate), annealed at 37°C for 1 h and stored at -20°C. For all knockdown experiments, 50 nM

133 siRNA transfections were conducted 2 days prior to infection or electroporation of viral RNAs.

134 Transfections were conducted using Lipofectamine RNAiMAX (Invitrogen) according to the

135 manufacturer's instructions with the modification that 20 µL of reagent were used to transfect a

136 10-cm dish of cells.

137

138 **HCV and VSV pseudoparticles (HCVpp and VSVpp)**

139 HCVpp consisting of a FLuc reporter lentiviral vector pseudotyped with the HCV E1 and E2

140 glycoprotein (from the H77 isolate, a genotype 1a strain) were a kind gift from John Law

141 (University of Alberta) (22). To generate lentiviral vectors pseudotyped with the VSV-G

142 glycoprotein (VSVpp), a 90% confluent 10-cm dish of 293T cells were transfected with 10 µg

143 pPRIME-FLuc, 5 µg psPAX.2, and 2.5 µg pVSV-G plasmid with 10 µL Lipofectamine 2000

144 (Invitrogen) diluted in 4 mL Opti-MEM. Media was changed 4, 20, and 28 h post-transfection.

145 At 48 h post-transfection, the cell culture media was passed through a 0.45 µm filter and stored
146 at -80°C.
147 To assay for cell entry, HCVpp and VSVpp were diluted 1/3 in dilution media (1X
148 DMEM, 3% FBS, 100 IU penicillin and 100 µg/mL streptomycin) with 20 mM HEPES and 4
149 µg/µL polybrene, and introduced to Huh-7.5 cells by spinoculation at 1,200 rpm for 1 h at room
150 temperature. The cells were left to recover at 37°C for at least 5 h before the pseudoparticle-
151 containing media was changed for fresh complete Huh-7.5 media. In parallel, cells seeded in a 6-
152 well plate were transfected with 1 µg of pPRIME-FLuc plasmid using Lipofectamine 2000
153 (Invitrogen) according to the manufacturer's instructions. Three days post-spinoculation and
154 transfection, cells were lysed in passive lysis buffer (Promega) and FLuc activity was assayed
155 using the Dual Reporter Luciferase kit (Promega).
156
157 **Infections**
158 Three days prior to infection, 10-cm dishes were seeded with 5 x $10^5$ Huh-7.5 cells, which were
159 transfected with siRNA duplexes on the following day. On the day of infection, each 10-cm dish
160 – containing approximately 1 x $10^6$ cells – was infected with 5 x $10^4$ FFU of JFH-$1_T$ diluted in 3
161 mL complete media. Four to five hours post-infection, each infected plate was split into three 10-
162 cm dishes. Protein, RNA, and virus samples were collected three days post-infection.
163
164 **Electroporations**
165 For each electroporation, 400 µL of resuspended cells (1.5 x $10^7$ cell/mL) were mixed with 2 µg
166 of FLuc mRNA and 5 µg of replicating (Δcore-p7 J6/JFH-1 RNA) or 10 µg GNN J6/JFH-1
167 RNA, and electroporated in 4-mm cuvettes at 270 V, 950 µF, and infinite resistance, optimized

168 for the Bio-Rad GenePulser XCell (Bio-Rad). Electroporated cells were resuspended in complete
169 Huh-7.5 media and transferred to 6-well plates for luciferase assays and protein analysis.
170
171 **Inhibition of RNA replication by 2´CMA**
172 Two days post-siRNA transfection, Huh-7.5 cells were infected with JFH-$1_T$ at a MOI of 0.05.
173 Four to five hours post-infection, each plate of infected cells was split into 6-well plates. Three
174 days post-infection, the media on these cells was changed for complete Huh-7.5 media with 5
175 μM 2´CMA (2´C-methyladenosine, Carbosynth), an HCV NS5B polymerase inhibitor, or DMSO
176 (vehicle control) (23). Total RNA and intracellular virus samples were collected at 0, 6 and 12 h
177 post-treatment, while cell culture supernatants were collected 6 and 12 h post-treatment. Protein
178 samples were collected from untreated plates to assess PCBP1 knockdown efficiency by Western
179 blot.
180
181 **Inhibition of virus secretion by Brefeldin A**
182 Three days post-infection with JFH-$1_T$, the cell culture media was replaced with complete Huh-
183 7.5 media with 5 μg/mL BFA (Brefeldin A, Biolegend) or equal volumes of DMSO (vehicle
184 control) (24). Total RNA, intracellular virus, and extracellular virus samples were collected at 0
185 and 6 h post-treatment. Protein samples were collected from untreated cells to verify PCBP1
186 knockdown by Western blot.
187
188 **Western blot analysis**
189 To collect total intracellular protein samples, cells were lysed in RIPA buffer (150 mM sodium
190 chloride, 1% NP-40, 0.5% sodium deoxycholate, 0.1% SDS, 50 mM Tris pH 8.0), supplemented

191 with Complete Protease Inhibitor Cocktail (Roche) and frozen at -80°C. Cellular debris was
192 pelleted by centrifugation at 16,000 x g for 30 min at 4°C, and the supernatant was quantified by
193 BCA Protein Assay (ThermoScientific). Ten micrograms of sample were loaded onto 10-12%
194 SDS-PAGE gels. Samples were transferred onto Immobilon-P PVDF membranes (Millipore),
195 blocked in 5% milk, and incubated overnight with primary antibodies diluted in 5% BSA: rabbit
196 anti-PCBP1 (clone EPR11055, Abcam ab168378, diluted 1:10,000); rabbit anti-actin (A2066,
197 Sigma, 1:20,000); mouse anti-HCV core (clone B2, Anogen MO-I40015B, 1:7,500); mouse anti-
198 JFH-1 NS5A (clone 7B5, BioFront Technologies, 1:10,000). Blots were incubated for 1 hour
199 with HRP-conjugated secondary antibodies diluted in 5% skim milk: anti-mouse (HAF007, R&D
200 Systems, 1:25,000); anti-rabbit (111-035-144, Jackson ImmunoResearch Laboratories, 1:50,000)
201 and visualized using enhanced chemiluminescence (ECL Prime Western Blotting Detection
202 Reagent, Fisher Scientific).
203
204 **RNA isolation and Northern blot analysis**
205 Total RNA was harvested using TRIzol Reagent (ThermoFisher Scientific) according to the
206 manufacturer's instructions. Ten micrograms of total RNA were separated on a 1% agarose gel
207 containing 1X 3-(N-morpholino)propanesulfonic acid (MOPS) buffer and 2.2 M formaldehyde
208 and transferred to a Zeta-probe membrane (Bio-Rad) by capillary transfer in 20X SSC buffer (3
209 M NaCl, 0.3 M sodium citrate). Membranes were hybridized in ExpressHyb Hybridization
210 Buffer (ClonTech) to random-primed $^{32}$P-labeled DNA probes (RadPrime DNA labelling
211 system, Life Technologies) complementary to HCV (nt 84-374) and γ-actin (nt 685-1171).
212 Autoradiograph band densities were quantified using Fiji (25).
213

214 **RT-qPCR analysis**

215 The iTaq Universal Probes One-Step kit (Bio-Rad) was used to perform duplex assays probing
216 for the HCV genome (NS5B-FW primer: 5'-AGACACTCCCCTATCAATTCATGGC-3';
217 NS5B-RV primer: 5'-GCGTCAAGCCCGTGTAACC-3'; NS5B-FAM probe: 5'-
218 ATGGGTTCGCATGGTCCTAATGACACAC-3') and the GAPDH loading control (PrimePCR
219 Probe assay with HEX probe, Bio-Rad). Each 20 µL reaction contained 500 ng of total RNA, 1.5
220 µL of the HCV primers and probe, and 0.5 µL of the GAPDH primers and probe. RT-PCR
221 reactions were conducted in a CFX96 Touch Deep Well Real-Time PCR system (Bio-Rad).
222 Genome copies were calculated using a standard curve and fold-differences in gene expression
223 were calculated using the $2^{-\Delta\Delta Ct}$ method (26).

224

225 **Luciferase assays**

226 For translation and replication assays, cells were washed in PBS and harvested in 100 µL of 1X
227 passive lysis buffer (Promega). The Dual-Luciferase Assay Reporter Kit (Promega) was used to
228 measure both *Renilla* and firefly luciferase activity according to the manufacturer's instructions
229 with the modification that 25 µL of reagent were used with 10 µL of sample. All samples were
230 measured in triplicate.

231

232 **Data analysis**

233 Statistical analyses were performed using GraphPad Prism v9 (GraphPad, USA). Statistical
234 significance was determined by paired t-test to compare results obtained from multiple
235 experiments, and by two-way ANOVA with Geisser-Greenhouse and Bonferroni corrections
236 when more than two comparisons were applied at once. To calculate half-lives, a one-step decay

237 curve using the least-squares regression was used, and error was reported as the asymmetrical
238 (profile likelihood) 95% confidence interval of the half-life. To calculate virus accumulation and
239 virus secretion rates, a simple linear regression was performed using the least squares regression
240 method. The slope and standard error calculated for each regression represents the rate of virus
241 accumulation or secretion.
242
243 **RESULTS**
244 **PCBP1 plays a role in the HCV life cycle**
245 Previous reports suggested that the PCBP1 protein directly interacted with the 5′ UTR of the
246 HCV genome, and a siRNA screen reported that PCBP1 knockdown reduced HCV RNA
247 accumulation (10, 16). Thus, we sought to further characterize the role of PCBP1 in the HCV life
248 cycle. Firstly, we assessed how PCBP1 knockdown affected the accumulation of HCVcc using
249 two viral strains: the cell culture-adapted JFH-$1_T$ strain (which has three adaptive mutations in
250 E2, p7, and NS2), and the chimeric J6/JFH-1 strain (where the coding region of the core through
251 to the first transmembrane domain of NS2 comes from the J6 sequence, and the remaining
252 sequences are derived from JFH-1) (**Figure 1A**) (17, 18). We found that knocking down
253 endogenous PCBP1 decreased viral protein expression and HCV RNA accumulation of both
254 strains, resulting in an approximately 2.2-fold and 3.3-fold decrease in JFH-$1_T$ and J6/JFH-1
255 viral RNA accumulation, respectively (**Figure 1B-D**). Quantification of intracellular virions
256 revealed no significant differences in JFH-$1_T$ titers between the PCBP1 knockdown and control
257 conditions; however, we observed an approximately 2.6-fold reduction in intracellular J6/JFH-1
258 titers during PCBP1 knockdown (**Figure 1E**). Surprisingly, when we quantified extracellular
259 virions, we observed that PCBP1 knockdown resulted in an overall increase in extracellular titers

260 of approximately 3.9-fold and 2.6-fold for JFH-$1_T$ and J6/JFH-1, respectively (**Figure 1F**).
261 Overall, PCBP1 knockdown increased the total quantity of virions produced by 3.7-fold for JFH-
262 $1_T$ and 2.1-fold for J6/JFH-1 (**Supplementary Figure S1**). To verify that this effect was
263 specifically due to the decrease in endogenous PCBP1 protein expression, we attempted to
264 rescue PCBP1 protein levels by ectopically expressing a siRNA-resistant PCBP1 with a N-
265 terminal FLAG tag (**Supplementary Figure S2**). Although we were unable to ectopically
266 express PCBP1 to the same level as the endogenous protein, we observed that ectopic PCBP1
267 expression diminished the impact of endogenous PCBP1 knockdown. Thus, in line with previous
268 findings, we found that PCBP1 knockdown decreased viral protein expression and intracellular
269 viral RNA accumulation. However, despite this overall decrease in viral protein and RNA
270 accumulation, we observed a marked increase in virion production and these effects were
271 partially reversed by ectopic expression of PCBP1.

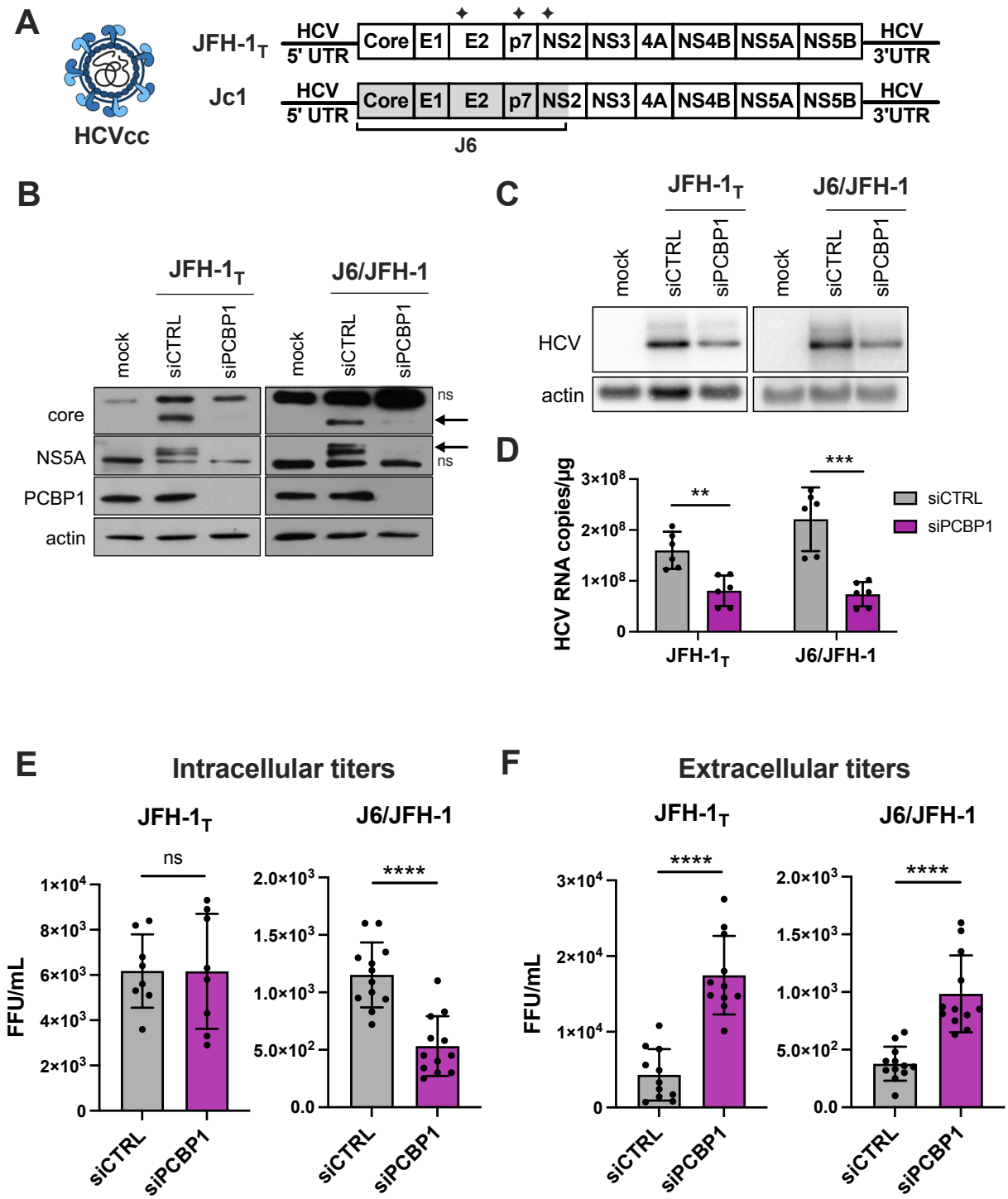


**Figure 1. PCBP1 knockdown decreases HCV protein expression and intracellular viral RNA accumulation, but increases secreted virus titers. (A)** Schematic representation of the

275 HCVcc infectious particles and genomic RNA used in infections. Huh-7.5 cells were transfected
276 with siPCBP1 or siCTRL two days prior to infection with JFH-$1_T$ or J6/JFH-1 (MOI = 0.05).
277 Total protein, RNA, and intracellular and extracellular infectious virus were harvested at day 3
278 post-infection. **(B)** Viral protein expression analysis by Western blot (ns, non-specific band;
279 arrow, core and NS5A bands). **(C)** Viral RNA accumulation analysis by Northern blot and **(D)**
280 quantification by RT-qPCR. **(E)** Intracellular and **(F)** extracellular (secreted) virus titers,
281 quantified by FFU assay. All data are representative of at least three independent biological
282 replicates, and error bars represent the standard deviation of the mean. Statistical significance
283 was calculated by paired t-test (ns, not significant; ** $p < 0.01$; *** $p < 0.001$; **** $p < 0.0001$).
284

285

286 **PCBP1 knockdown does not have a direct impact on HCV entry, translation, genome**
287 **stability or viral RNA replication**

288 To clarify PCBP1's precise role(s) in the HCV life cycle, we used assays to specifically examine
289 different steps of the viral life cycle (**Figure 2**). Firstly, we explored whether PCBP1 knockdown
290 had an effect on viral entry using the HCV pseudoparticle (HCVpp) system. HCVpp are
291 lentiviral vectors with a firefly luciferase reporter gene pseudotyped with the HCV E1 and E2
292 glycoproteins (22). HCVpp engage with HCV-specific entry receptors, then enter cells by
293 clathrin-mediated endocytosis; thus, to account for any changes in clathrin-mediated endocytosis,
294 we used vesicular stomatitis virus (VSV) pseudoparticles (VSVpp) as a control. In addition, to
295 verify that PCBP1 knockdown did not affect luciferase reporter gene expression, we assessed
296 firefly luciferase expression from cells directly transfected with a FLuc reporter plasmid. In all
297 cases, we found that depletion of endogenous PCBP1 had no impact on luciferase activity
298 (**Figure 2A**). This suggests that PCBP1 knockdown does not affect FLuc reporter expression,
299 clathrin-mediated endocytosis, or HCVpp entry.

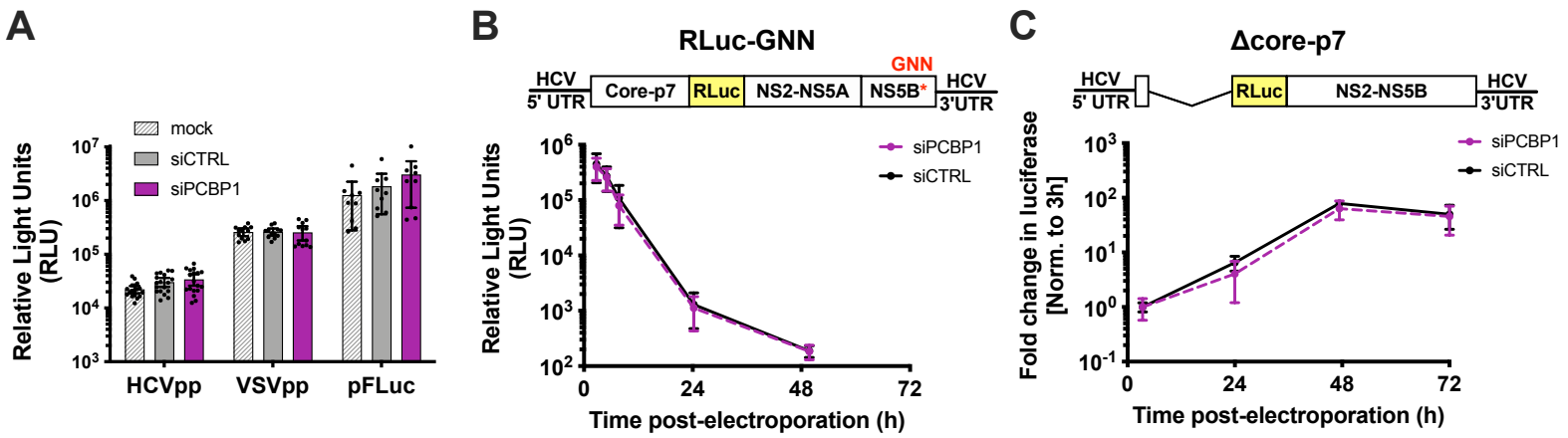


**Figure 2. PCBP1 knockdown has no direct effect on HCV entry, translation, genome stability or RNA replication. (A)** siRNA-transfected Huh-7.5 cells were spinoculated with luciferase reporter pseudoparticles expressing the HCV E1/E2 glycoproteins (HCVpp) or the VSV-G glycoprotein (VSVpp). In parallel, cells were transfected with a firefly luciferase expression plasmid. Samples were harvested 3 days post-infection/transfection and analyzed by luciferase assay. **(B)** siRNA-transfected Huh-7.5 cells were electroporated with replication-defective J6/JFH-1-RLuc-GNN RNAs, and luciferase activity was monitored at several timepoints in the two days post-electroporation. **(C)** Huh-7.5 cells were electroporated with the replication-competent Δcore-p7 J6/JFH RLuc RNA, and luciferase activity was monitored at several timepoints post-electroporation. RLuc values were normalized to the early timepoint (3h), to control for disparities in electroporation efficiency between experiments. All data are representative of at least three independent biological replicates and error bars represent the standard deviation of the mean.

To examine PCBP1's impact on viral translation, we used a full-length J6/JFH-1 RLuc reporter RNA containing an inactivating mutation in the NS5B polymerase gene (GNN). The RLuc activity thus served as a direct measure of HCV IRES-mediated translation, and over time, this signal also served as a proxy measure for viral RNA stability. We found that the PCBP1 knockdown and control conditions had similar RLuc activity at all timepoints (**Figure 2B**).

320 Moreover, the luciferase signal half-lives were nearly identical, with 2.68 h (95% CI 1.64 – 4.64)
321 and 2.71 h (95% CI 1.43 – 5.50) for the PCBP1 knockdown and control conditions, respectively.
322 Thus, PCBP1 knockdown does not directly impact either HCV IRES-mediated translation or
323 genome stability.
324 To assess the impact of PCBP1 knockdown on HCV RNA replication, we made use of a
325 J6/JFH-1 subgenomic replicon RLuc reporter RNA, with a deletion of the structural proteins
326 (Δcore-p7), which allowed us to assess viral RNA replication in the absence of virion assembly
327 (**Figure 2C**). We observed no significant differences in subgenomic replicon RNA accumulation
328 during PCBP1 knockdown compared with control conditions, suggesting that PCBP1
329 knockdown does not affect viral RNA replication. Interestingly, we also observed no significant
330 differences in luciferase activity during PCBP1 knockdown and control conditions of a full-
331 length WT J6/JFH-1 RLuc genomic RNA or of a full-length J6/JFH-1 genomic RNA containing
332 a GFP insertion in the NS5A gene (NS5A-GFP), which was previously shown to impair virion
333 assembly without impairing viral RNA replication (**Supplementary Figure S3**) (6, 27). While
334 this is seemingly in contrast to our findings with HCVcc, where PCBP1 depletion decreased viral
335 RNA levels (**Figure 1C and D**); it is important to note that all of these reporter viral RNAs are
336 defective in viral packaging due to the large RLuc reporter gene insertion, which results in >100-
337 to >1000-fold reductions in infectious virion production (**Supplementary Figure S3**). Thus,
338 taken together, our data suggests that PCBP1 knockdown does not have a direct effect on viral
339 RNA replication.
340

341 **PCBP1 knockdown limits virus secretion**

342 As we had found that silencing PCBP1 did not have a significant impact on HCV entry,
343 translation, genome stability or viral RNA replication, we reasoned that PCBP1 was likely to be
344 exerting an effect on virion assembly and/or secretion. To investigate this possibility, we used a
345 nucleoside analog, 2´C-methyladenosine (2´CMA), to block viral RNA synthesis by the HCV
346 NS5B RNA-dependent RNA polymerase and monitored virion production over time (**Figure 3**)
347 (23). Similar to related studies using Zika virus, we reasoned that blocking viral RNA synthesis
348 could allow us to assess if PCBP1 knockdown modulated viral assembly and secretion in the
349 absence of genomic RNA production (28). To this end, we infected cells with JFH-$1_T$ and, three
350 days post-infection, treated cells with 2´CMA or vehicle (DMSO), and monitored viral RNA
351 accumulation as well as intracellular and extracellular virion production over the next 12 hours
352 (**Figure 3A**). In agreement with our previous findings, we observed an overall reduction in JFH-
353 $1_T$ viral RNA accumulation by day 3 post-infection during PCBP1 knockdown (0 h timepoint,
354 **Figure 3B**). In addition, 2´CMA treatment efficiently blocked further viral RNA accumulation,
355 which continued to increase under the vehicle (DMSO) condition (6-12 h timepoints, **Figure**
356 **3B**). We observed that intracellular viral titers were initially similar in both PCBP1 knockdown
357 and control conditions, but that infectious virions accumulated at a slightly faster rate during
358 PCBP1 knockdown in DMSO-treated cells (**Figure 3C and D**). In contrast, the 2´CMA
359 treatment induced a similar decrease in intracellular titers during both PCBP1 knockdown and
360 control conditions, resulting in similar rates of intracellular virion accumulation (**Figure 3C and**
361 **D**). Interestingly, as we had observed previously (**Figure 1F**), PCBP1 knockdown resulted in an
362 increase in extracellular titers which continued upon 2´CMA treatment (**Figure 3E and F**).
363 Despite an overall reduction in extracellular virion production during 2´CMA treatment, we
364 observed that PCBP1 knockdown still resulted in higher extracellular titers and virion secretion
365 rates than the control condition under both 2´CMA and vehicle (DMSO) treatment (**Figure 3E**
366 **and F**). Taken together, these results suggest that endogenous PCBP1 typically limits the
367 secretion of infectious viral particles during the HCV life cycle.

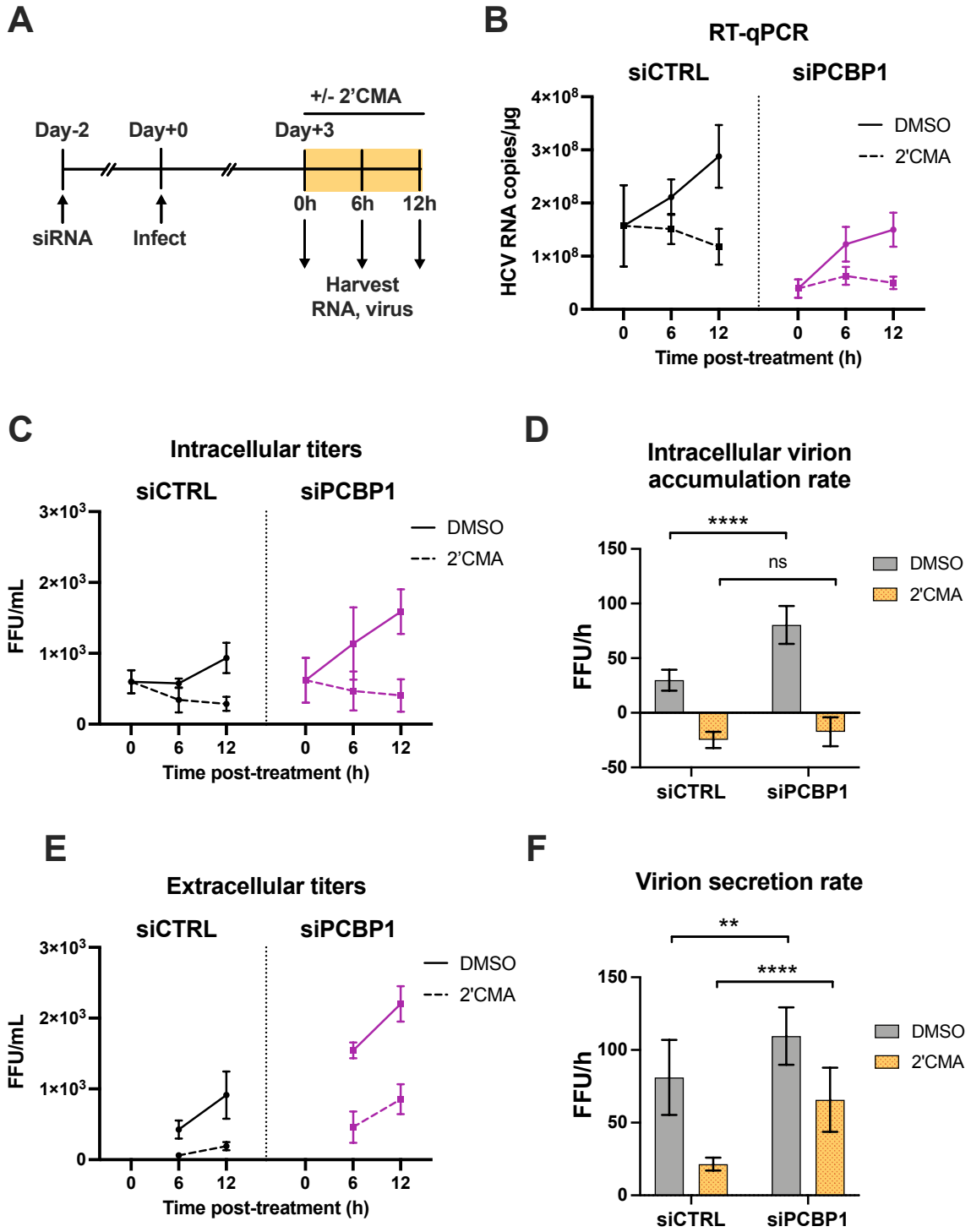


**Figure 3. PCBP1 knockdown enhances infectious virion secretion even in the absence of RNA replication**. **(A)** Schematic representation of the experimental approach for 2´CMA experiments: two days post-siRNA transfection, Huh-7.5 cells were infected with JFH-$1_T$ (MOI = 0.05). Three days post-infection, the cell culture medium was replaced with media containing

372 2´CMA or DMSO (vehicle control). Total RNA, intracellular and extracellular virus were
373 collected at t = 0, 6 and 12 h post-treatment. **(B)** Quantitative RT-PCR analysis after 2´CMA
374 treatment. **(C)** Intracellular viral titers and **(D)** intracellular virus accumulation rate calculated by
375 linear regression. **(E)** Extracellular viral titers and **(F)** virus secretion rates calculated by linear
376 regression. All data are representative of three independent replicates and error bars in (B), (C)
377 and (E) represent the standard deviation of the mean. Error bars in (D) and (F) represent the
378 slopes of the linear regressions ± standard error. Statistical significance was calculated by two-
379 way ANOVA. (ns, not significant; ** $p < 0.01$; **** $p < 0.0001$).
380

381 **Blocking virion secretion partially restores HCV RNA accumulation during PCBP1**
382 **knockdown**

383 During virion secretion, viral genomes that have been packaged into new infectious particles are
384 removed from the cell. Since our previous findings suggested that PCBP1 knockdown increases
385 virion secretion, we wondered if this increased egress of assembled viral particles (packaged
386 viral genomic RNAs) might explain our initial observation that PCBP1 knockdown led to an
387 overall reduction in viral RNA accumulation (**Figure 1C-D**). To directly test this, we treated
388 HCV-infected cells with Brefeldin A (BFA), a protein trafficking inhibitor previously shown to
389 prevent HCV virion secretion (**Figure 4**) (24). As previously reported, we found that BFA
390 treatment blocked the secretion of infectious virions, resulting in a sharp decline in extracellular
391 titers and an increase in intracellular titers relative to untreated cells or to vehicle (DMSO)
392 treatment (**Figure 4A and B**). Consistent with our prior results, PCBP1 knockdown resulted in a
393 greater than 2-fold decrease in viral RNA accumulation, while BFA treatment resulted in a
394 partial rescue of HCV RNA accumulation during PCBP1 knockdown (**Figure 4C**). Thus,

395 blocking cellular secretory pathways, thereby preventing virion secretion, can partially rescue

396 intracellular viral RNA accumulation defects resultant from PCBP1 knockdown.

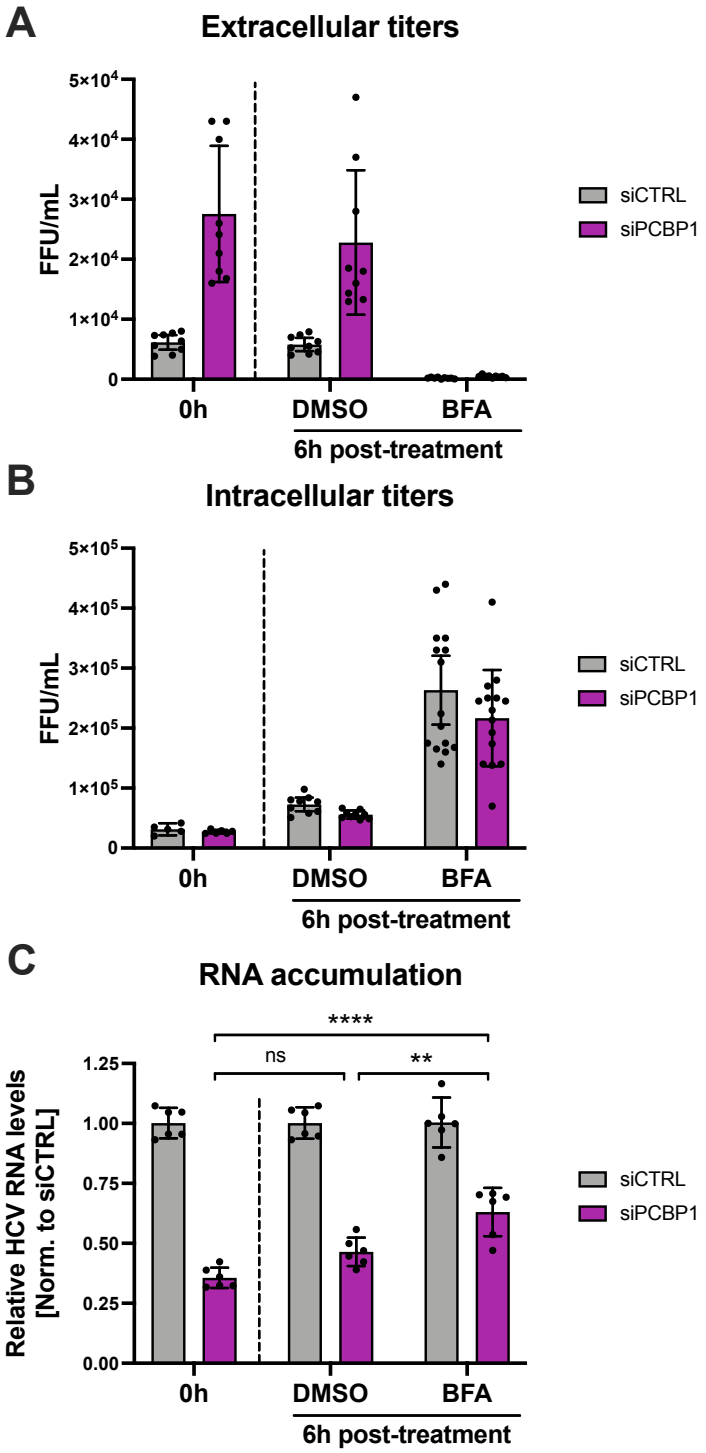

397 **Figure 4. Blocking HCV secretion partially rescues intracellular RNA accumulation during**
398 **PCBP1 knockdown.** Three days post-JFH-$1_T$ infection (MOI 0.05), the cell culture medium was
399 replaced with media containing Brefeldin A (BFA) or DMSO (vehicle control). Total
400 intracellular RNA, intracellular virus, and extracellular virus were collected at 0 h and 6 h post-
401 treatment. **(A)** Extracellular (secreted) viral titers and **(B)** intracellular viral titers from untreated
402 cells (0h) and after 6h of DMSO or BFA treatment, quantified by FFU assay. **(C)** Intracellular
403 RNA accumulation relative to the siCTRL condition, assessed by RT-qPCR analysis. All data
404 are representative of three independent biological replicates, and error bars represent the standard
405 deviation of the mean. Statistical significance was calculated by paired t-test (ns, not significant;
406 ** $p < 0.01$; **** $p < 0.0001$).

407

408 **DISCUSSION**

409 Herein, we investigated the role of PCBP1 in the HCV life cycle. Previous studies had found that
410 PCBP1 interacts with the HCV 5′ UTR *in vitro* (10, 15), and that PCBP1 silencing inhibited
411 HCV RNA accumulation in cell culture (16), yet the precise steps of the HCV life cycle
412 modulated by PCBP1 remained unclear. Our systematic evaluation of the effects of PCBP1
413 knockdown on individual steps of the viral life cycle revealed that PCBP1 depletion did not
414 directly affect virus entry, translation, genome stability or viral RNA replication, but rather
415 resulted in increased infectious virion production in cell culture. Specifically, PCBP1
416 knockdown significantly increased virion secretion, resulting in the depletion of intracellular
417 viral RNA. Additionally, inhibiting virion secretion could partially restore HCV RNA
418 accumulation during PCBP1 knockdown. Thus, our findings suggest a model whereby
419 endogenous PCBP1 normally limits virion assembly and secretion, such that viral genomes
420 remain available to engage in the translation and replication steps of the viral life cycle (**Figure**
421 **5**). As such, PCBP1 depletion increases the proportion of viral genomes engaged in virion

422 assembly and secretion, which decreases the pool of translating/replicating viral RNAs. We
423 anticipate that these differences in intracellular viral RNA levels would compound over time,
424 with PCBP1-replete cells rapidly increasing their pool of intracellular viral RNA through
425 repeated cycles of translation and RNA replication, while the smaller pool of
426 translating/replicating RNAs in PCBP1-depleted cells would result in a much slower rate of viral
427 RNA accumulation over time.
428

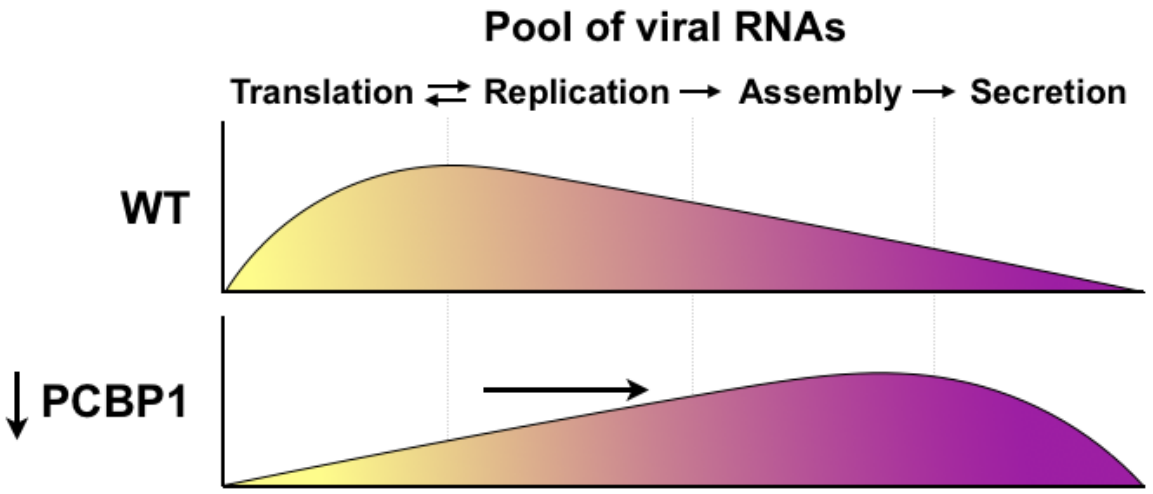


429 **Figure 5. Model for PCBP1's effects on HCV assembly and secretion.** Under wild-type
430 conditions, endogenous PCBP1 limits HCV assembly and secretion, and the majority of
431 intracellular viral RNAs are engaged in translation and viral genome replication. In contrast,
432 PCBP1 knockdown promotes virion assembly and secretion. This results in a shift in viral RNA
433 utilization such that an increased proportion of viral RNAs are engaged in viral particle
434 production, leaving a smaller proportion of viral RNAs to engage in the translating/replicating
435 pool.
436
437
438 Notably, most of the experiments conducted herein made use of JFH-$1_T$, a cell culture-
439 adapted strain that produces greater yields of infectious virions in cell culture than the parental

440 JFH-1 strain (5, 17). To verify that the phenotype we observed was not an artefact of the JFH-$1_T$
441 strain itself, we validated our findings with J6/JFH-1, a chimeric virus that is widely used in
442 HCVcc studies, commonly referred to as Jc1 (18). Knockdown of PCBP1 had a similar effect on
443 JFH-$1_T$ and J6/JFH-1 protein expression, RNA accumulation, and extracellular viral titers;
444 however, we found that while JFH-$1_T$ intracellular titers were not significantly different from
445 control condition, J6/JFH-1 intracellular titers were significantly decreased by approximately
446 2.6-fold (**Figure 1E**). Nonetheless, PCBP1 knockdown still resulted in an overall greater than 2-
447 fold increase in the total number of infectious virions produced by both strains (**Supplementary**
448 **Figure S1**). Since an infectious viral particle must have undergone the process of virion
449 assembly, this suggests that PCBP1 depletion enhances the assembly of infectious virions in
450 addition to their subsequent secretion. Importantly, this data could reflect pre-existing strain
451 differences in virion assembly, as J6/JFH-1 has previously been reported to be more efficient
452 than JFH-1 in virion assembly (29, 30). Specifically, the J6 core protein was shown to localize
453 closer to the sites of virion assembly on the endoplasmic reticulum (ER) than the JFH-1 core
454 protein, which accumulates to a greater extent on lipid droplets (29, 30). Furthermore, J6/JFH-1
455 allocates a greater proportion of its viral genomes to virion assembly than JFH-1, which allocates
456 more viral RNAs to the translating/replicating pool (29, 30). Thus, it is possible that PCBP1
457 knockdown promotes both the assembly and secretion of J6/JFH-1 virions, but minor gains in the
458 already efficient virion assembly step are less apparent than the gains in virion secretion for this
459 particular strain.

460 Interestingly, PCBP1 has also been previously implicated in attenuation of antiviral
461 signalling, specifically in the regulation and turnover of MAVS, a signal transduction protein
462 directly downstream of RIG-I, which is known to limit HCV infection (31). However, all of our

463 conclusions were drawn from experiments conducted in the Huh-7.5 cell line, which has well-
464 documented defects in the RIG-I antiviral signalling pathway (32). Additionally, our own brief
465 explorations of interferon induction and MAVS turnover did not reveal any significant
466 differences between PCBP1 knockdown and control conditions (data not shown). Moreover, the
467 HCV NS3-4A protease also inactivates MAVS during infection to reduce antiviral signaling and
468 recognition of the viral RNA (33, 34). However, as hepatocytes typically express RIG-I and
469 MAVS, we cannot rule out the possibility that PCBP1 may also modulate this pathway during
470 infection *in vivo*.

471 Finally, PCBP1's closely related paralogs, hnRNP K and PCBP2, have been more
472 extensively studied during HCV infection. While the hnRNP K protein was shown to restrict
473 infectious virion production, the PCBP2 protein has been suggested to modulate viral translation
474 and RNA replication (13, 14). Since the PCBP1 amino acid identity is far more similar to PCBP2
475 (~80% identity) than hnRNP K (~24% identity), we were initially surprised that our findings for
476 PCBP1 in HCV infection closely matched those reported for hnRNP K. Yet, while PCBP1 and
477 PCBP2 have been shown to perform similar functions, they have also been reported to play
478 distinct roles during poliovirus, vesicular stomatitis virus, and human immunodeficiency virus
479 infection (35-37). In addition to the similarities we observed between PCBP1 and the effects
480 previously reported for hnRNP K, our results and conclusions also echo those reported for the
481 IGF2BP2/YBX-1 complex, METTL3/METTL14 *N*6-methyladenosine ($m^6A$) writers, and the
482 YTHDF $m^6A$-binding proteins during HCV infection (13, 38, 39). All of these complexes have
483 been reported to inhibit HCV infectious particle production, with no effect on viral translation or
484 RNA replication – with the exception of the IGF2BP2/YBX-1 complex, which plays an
485 additional role in facilitating viral RNA replication (38). It is currently unclear if PCBP1, hnRNP

486 K, the YBX-1 complex, or $m^6A$ modification of the HCV genome inhibit virion assembly as
487 components of a common pathway, or through distinct and/or additive mechanisms.
488 Interestingly, high-throughput affinity capture and proximity ligation studies have found that
489 PCBP1 interacts with hnRNP K, IGF2BP2, YBX-1, METTL3 and METTL14; although this has
490 been demonstrated only in non-hepatic cell lines to date (40-42). Should these interactions be
491 conserved during HCV infection, it seems plausible that PCBP1 may participate in one or more
492 of these complexes which together inhibit HCV virion assembly and secretion. Future
493 investigations will thus be needed to reveal whether these proteins function in an overlapping or
494 distinct manner; and, are likely to further improve our understanding of HCV virion assembly as
495 well as how this process is regulated by cellular RNA binding proteins.
496 In conclusion, our results support a model whereby endogenous PCBP1 limits HCV
497 infectious particle production. By preventing virion assembly and secretion, PCBP1 indirectly
498 enhances viral RNA accumulation. The model presented herein helps to inform our
499 understanding of how cellular RNA-binding proteins modulate HCV genomic RNA utilization
500 during the viral life cycle, specifically as it pertains to virion assembly. While the precise
501 molecular mechanism(s) employed by PCBP1 to inhibit HCV assembly and egress remain to be
502 characterized, similar phenotypes reported for hnRNP K, IGF2BP2/YBX-1 and $m^6A$
503 modification of the HCV genome offer promising leads for future investigations.

504 **ACKNOWLEDGEMENTS**

505 We would like to acknowledge Charlie Rice (Rockefeller University) for kindly providing the
506 Huh-7.5 cells, pJ6/JFH (pJc1), pJ6/JFH FL RLuc WT and GNN plasmids; Rodney Russell
507 (Memorial University) for providing JFH-$1_T$; Mamata Panigrahi and Joyce Wilson (University of
508 Saskatchewan) for the pJ6/JFH mono RLuc NS2 ("Δcore-p7") plasmid; Martin J Richer (McGill
509 University) for the 293T cells; John Law (University of Alberta) for the kind gift of HCVpp. We
510 are also grateful to Nathan Taylor, Julie Magnus, and Carolina Camargo (McGill University) for
511 technical support, and to Craig McCormick's graduate journal club (Dalhousie University) for
512 their critical feedback on a previous iteration of this manuscript.

513

514 **FUNDING INFORMATION**

515 This research was supported by the Canadian Institutes for Health Research (CIHR) [MOP-
516 136915 and PJT-169214]. S.E.C. was supported by the Canadian Network on Hepatitis C
517 (CanHepC) training program, as well as a Vanier Canada Graduate Scholarship. M.R. was also
518 supported by the CanHepC training program. In addition, this research was undertaken, in part,
519 thanks to the Canada Research Chairs program (S.M.S.).

520

521 **AUTHOR CONTRIBUTIONS**

522 S.E.C. and S.M.S. designed the study; S.E.C. and M.R. performed the experiments and analyzed
523 the data, and S.E.C and S.M.S. wrote and edited the manuscript.

524 **REFERENCES**


525 1. **Tsukiyama-Kohara K**, **Iizuka N**, **Kohara M**, **Nomoto A**. 1992. Internal ribosome entry
526 site within hepatitis C virus RNA. Journal of Virology **66**:1476–1483.

527 2. **Lancaster AM**, **Jan E**, **Sarnow P**. 2006. Initiation factor-independent translation
528 mediated by the hepatitis C virus internal ribosome entry site. RNA **12**:894–902.

529 3. **Lohmann V**, **Korner F**, **Koch J**, **Herian U**, **Theilmann L**, **Bartenschlager R**. 1999.
530 Replication of subgenomic hepatitis C virus RNAs in a hepatoma cell line. Science
531 **285**:110–113.

532 4. **Jones CT**, **Murray CL**, **Eastman DK**, **Tassello J**, **Rice CM**. 2007. Hepatitis C virus p7
533 and NS2 proteins are essential for production of infectious virus. Journal of Virology
534 **81**:8374–8383.

535 5. **Jones DM**, **Atoom AM**, **Zhang X**, **Kottilil S**, **Russell RS**. 2011. A genetic interaction
536 between the core and NS3 proteins of hepatitis C virus is essential for production of
537 infectious virus. Journal of Virology **85**:12351–12361.

538 6. **Masaki T**, **Suzuki R**, **Murakami K**, **Aizaki H**, **Ishii K**, **Murayama A**, **Date T**,
539 **Matsuura Y**, **Miyamura T**, **Wakita T**, **Suzuki T**. 2008. Interaction of hepatitis C virus
540 nonstructural protein 5A with core protein is critical for the production of infectious virus
541 particles. Journal of Virology **82**:7964–7976.

542 7. **Appel N**, **Zayas M**, **Miller S**, **Krijnse-Locker J**, **Schaller T**, **Friebe P**, **Kallis S**, **Engel**
543 **U**, **Bartenschlager R**. 2008. Essential role of domain III of nonstructural protein 5A for
544 hepatitis C virus infectious particle assembly. PLoS Pathog **4**:e1000035.

545 8. **Matunis MJ**, **Michael WM**, **Dreyfuss G**. 1992. Characterization and primary structure of
546 the poly(C)-binding heterogeneous nuclear ribonucleoprotein complex K protein. Mol
547 Cell Biol **12**:164–171.

548 9. **Du Z**, **Lee JK**, **Fenn S**, **Tjhen R**, **Stroud RM**, **James TL**. 2007. X-ray crystallographic
549 and NMR studies of protein-protein and protein-nucleic acid interactions involving the
550 KH domains from human poly(C)-binding protein-2. RNA **13**:1043–1051.

551 10. **Spångberg K**, **Schwartz S**. 1999. Poly(C)-binding protein interacts with the hepatitis C
552 virus 5' untranslated region **80**:1371–1376.

553 11. **Flynn RA**, **Martin L**, **Spitale RC**, **Do BT**, **Sagan SM**, **Zarnegar B**, **Qu K**, **Khavari PA**,
554 **Quake SR**, **Sarnow P**, **Chang HY**. 2015. Dissecting noncoding and pathogen RNA-
555 protein interactomes. RNA **21**:135–143.

556 12. **Fan B**, **Lu K-Y**, **Reymond Sutandy FX**, **Chen Y-W**, **Konan K**, **Zhu H**, **Kao CC**, **Chen**
557 **C-S**. 2014. A human proteome microarray identifies that the heterogeneous nuclear

558 ribonucleoprotein K (hnRNP K) recognizes the 5' terminal sequence of the hepatitis C
559 virus RNA. Mol Cell Proteomics **13**:84–92.

560 13. **Poenisch M**, **Metz P**, **Blankenburg H**, **Ruggieri A**, **Lee J-Y**, **Rupp D**, **Rebhan I**,
561 **Diederich K**, **Kaderali L**, **Domingues FS**, **Albrecht M**, **Lohmann V**, **Erfle H**,
562 **Bartenschlager R**. 2015. Identification of HNRNPK as Regulator of Hepatitis C Virus
563 Particle Production. PLoS Pathog **11**:e1004573–21.

564 14. **Wang L**, **Jeng K-S**, **Lai MMC**. 2011. Poly(C)-binding protein 2 interacts with sequences
565 required for viral replication in the hepatitis C virus (HCV) 5' untranslated region and
566 directs HCV RNA replication through circularizing the viral genome. Journal of Virology
567 **85**:7954–7964.

568 15. **Choi K**, **Kim JH**, **Li X**, **Paek KY**, **Ha SH**, **Ryu SH**, **Wimmer E**, **Jang SK**. 2004.
569 Identification of cellular proteins enhancing activities of internal ribosomal entry sites by
570 competition with oligodeoxynucleotides. Nucleic Acids Research **32**:1308–1317.

571 16. **Randall G**, **Panis M**, **Cooper JD**, **Tellinghuisen TL**, **Sukhodolets KE**, **Pfeffer S**,
572 **Landthaler M**, **Landgraf P**, **Kan S**, **Lindenbach BD**, **Chien M**, **Weir DB**, **Russo JJ**, **Ju**
573 **J**, **Brownstein MJ**, **Sheridan R**, **Sander C**, **Zavolan M**, **Tuschl T**, **Rice CM**. 2007.
574 Cellular cofactors affecting hepatitis C virus infection and replication. PNAS **104**:12884–
575 12889.

576 17. **Russell RS**, **Meunier J-C**, **Takikawa S**, **Faulk K**, **Engle RE**, **Bukh J**, **Purcell RH**,
577 **Emerson SU**. 2008. Advantages of a single-cycle production assay to study cell culture-
578 adaptive mutations of hepatitis C virus. Proc Natl Acad Sci USA **105**:4370–4375.

579 18. **Pietschmann T**, **Kaul A**, **Koutsoudakis G**, **Shavinskaya A**, **Kallis S**, **Steinmann E**,
580 **Abid K**, **Negro F**, **Dreux M**, **Cosset F-L**, **Bartenschlager R**. 2006. Construction and
581 characterization of infectious intragenotypic and intergenotypic hepatitis C virus chimeras.
582 PNAS **103**:7408–7413.

583 19. **Panigrahi M**, **Thibault PA**, **Wilson JA**. 2021. miR-122 affects both the initiation and
584 maintenance of Hepatitis C Virus infections. bioRxiv [preprint] 1–43.

585 20. **Amador-Cañizares Y**, **Bernier A**, **Wilson JA**, **Sagan SM**. 2018. miR-122 does not
586 impact recognition of the HCV genome by innate sensors of RNA but rather protects the
587 5′ end from the cellular pyrophosphatases, DOM3Z and DUSP11. Nucleic Acids Research
588 **46**:5139–5158.

589 21. **Machlin ES**, **Sagan SM**, **Sarnow P**. 2011. Masking the 5' terminal nucleotides of the
590 hepatitis C virus genome by an unconventional microRNA-target RNA complex. PNAS
591 **108**:3193–3198.

592 22. **Hsu M**, **Zhang J**, **Flint M**, **Logvinoff C**, **Cheng-Mayer C**, **Rice CM**, **McKeating JA**.
593 2003. Hepatitis C virus glycoproteins mediate pH-dependent cell entry of pseudotyped
594 retroviral particles. PNAS **100**:7271–7276.

595 23. **Carroll SS**, **Tomassini JE**, **Bosserman M**, **Getty K**, **Stahlhut MW**, **Eldrup AB**, **Bhat**
596 **B**, **Hall D**, **Simcoe AL**, **LaFemina R**, **Rutkowski CA**, **Wolanski B**, **Yang Z**, **Migliaccio**
597 **G**, **De Francesco R**, **Kuo LC**, **MacCoss M**, **Olsen DB**. 2003. Inhibition of hepatitis C
598 virus RNA replication by 2'-modified nucleoside analogs. Journal of Biological Chemistry
599 **278**:11979–11984.

600 24. **Gastaminza P**, **Cheng G**, **Wieland S**, **Zhong J**, **Liao W**, **Chisari FV**. 2008. Cellular
601 determinants of hepatitis C virus assembly, maturation, degradation, and secretion. Journal
602 of Virology **82**:2120–2129.

603 25. **Schindelin J**, **Arganda-Carreras I**, **Frise E**, **Kaynig V**, **Longair M**, **Pietzsch T**,
604 **Preibisch S**, **Rueden C**, **Saalfeld S**, **Schmid B**, **Tinevez J-Y**, **White DJ**, **Hartenstein V**,
605 **Eliceiri K**, **Tomancak P**, **Cardona A**. 2012. Fiji: an open-source platform for biological-
606 image analysis. Nat Meth **9**:676–682.

607 26. **Livak KJ**, **Schmittgen TD**. 2001. Analysis of Relative Gene Expression Data Using
608 Real-Time Quantitative PCR and the 2−ΔΔCT Method. Methods **25**:402–408.

609 27. **Moradpour D**, **Evans MJ**, **Gosert R**, **Yuan Z**, **Blum HE**, **Goff SP**, **Lindenbach BD**,
610 **Rice CM**. 2004. Insertion of green fluorescent protein into nonstructural protein 5A
611 allows direct visualization of functional hepatitis C virus replication complexes. Journal of
612 Virology **78**:7400–7409.

613 28. **Taguwa S**, **Yeh M-T**, **Rainbolt TK**, **Nayak A**, **Shao H**, **Gestwicki JE**, **Andino R**,
614 **Frydman J**. 2019. Zika Virus Dependence on Host Hsp70 Provides a Protective Strategy
615 against Infection and Disease. CellReports **26**:906–920.e3.

616 29. **Boson B**, **Granio O**, **Bartenschlager R**, **Cosset F-L**. 2011. A concerted action of
617 hepatitis C virus p7 and nonstructural protein 2 regulates core localization at the
618 endoplasmic reticulum and virus assembly. PLoS Pathog **7**:e1002144.

619 30. **Iwanami S**, **Kitagawa K**, **Ohashi H**, **Asai Y**, **Shionoya K**, **Saso W**, **Nishioka K**, **Inaba**
620 **H**, **Nakaoka S**, **Wakita T**, **Diekmann O**, **Iwami S**, **Watashi K**. 2020. Should a viral
621 genome stay in the host cell or leave? A quantitative dynamics study of how hepatitis C
622 virus deals with this dilemma. PLoS Biol **18**:e3000562–17.

623 31. **Zhou X**, **You F**, **Chen H**, **Jiang Z**. 2012. Poly(C)-binding protein 1 (PCBP1) mediates
624 housekeeping degradation of mitochondrial antiviral signaling (MAVS). Cell Res **22**:717–
625 727.

626 32. **Sumpter R**, **Loo Y-M**, **Foy E**, **Li K**, **Yoneyama M**, **Fujita T**, **Lemon SM**, **Gale M**.
627 2005. Regulating intracellular antiviral defense and permissiveness to hepatitis C virus
628 RNA replication through a cellular RNA helicase, RIG-I. Journal of Virology **79**:2689–
629 2699.

630 33. **Meylan E**, **Curran J**, **Hofmann K**, **Moradpour D**, **Binder M**, **Bartenschlager R**,
631 **Tschopp J**. 2005. Cardif is an adaptor protein in the RIG-I antiviral pathway and is
632 targeted by hepatitis C virus. Nature **437**:1167–1172.

633 34. **Bender S**, **Reuter A**, **Eberle F**, **Einhorn E**, **Binder M**, **Bartenschlager R**. 2015.
634 Activation of Type I and III Interferon Response by Mitochondrial and Peroxisomal
635 MAVS and Inhibition by Hepatitis C Virus. PLoS Pathog **11**:e1005264–30.

636 35. **Walter BL**, **Parsley TB**, **Ehrenfeld E**, **Semler BL**. 2002. Distinct Poly(rC) Binding
637 Protein KH Domain Determinants for Poliovirus Translation Initiation and Viral RNA
638 Replication. Journal of Virology **76**:12008–12022.

639 36. **Dinh PX**, **Beura LK**, **Panda D**, **Das A**, **Pattnaik AK**. 2011. Antagonistic effects of
640 cellular poly(C) binding proteins on vesicular stomatitis virus gene expression. Journal of
641 Virology, 3rd ed. **85**:9459–9471.

642 37. **Woolaway K**, **Asai K**, **Emili A**, **Cochrane A**. 2007. hnRNP E1 and E2 have distinct roles
643 in modulating HIV-1 gene expression. Retrovirology **4**:28–18.

644 38. **Chatel-Chaix L**, **Germain M-A**, **Motorina A**, **Bonneil É**, **Thibault P**, **Baril M**,
645 **Lamarre D**. 2013. A host YB-1 ribonucleoprotein complex is hijacked by hepatitis C
646 virus for the control of NS3-dependent particle production. Journal of Virology **87**:11704–
647 11720.

648 39. **Gokhale NS**, **McIntyre ABR**, **McFadden MJ**, **Roder AE**, **Kennedy EM**, **Gandara JA**,
649 **Hopcraft SE**, **Quicke KM**, **Vazquez C**, **Willer J**, **Ilkayeva OR**, **Law BA**, **Holley CL**,
650 **Garcia-Blanco MA**, **Evans MJ**, **Suthar MS**, **Bradrick SS**, **Mason CE**, **Horner SM**.
651 2016. N6-Methyladenosine in Flaviviridae Viral RNA Genomes Regulates Infection. Cell
652 Host & Microbe **20**:654–665.

653 40. **Rosenbluh J**, **Mercer J**, **Shrestha Y**, **Oliver R**, **Tamayo P**, **Doench JG**, **Tirosh I**,
654 **Piccioni F**, **Hartenian E**, **Horn H**, **Fagbami L**, **Root DE**, **Jaffe J**, **Lage K**, **Boehm JS**,
655 **Hahn WC**. 2016. Genetic and Proteomic Interrogation of Lower Confidence Candidate
656 Genes Reveals Signaling Networks in β-Catenin-Active Cancers. Cell Syst **3**:302–316.e4.

657 41. **Youn J-Y**, **Dunham WH**, **Hong SJ**, **Knight JDR**, **Bashkurov M**, **Chen GI**, **Bagci H**,
658 **Rathod B**, **MacLeod G**, **Eng SWM**, **Angers S**, **Morris Q**, **Fabian M**, **Côté J-F**,
659 **Gingras A-C**. 2018. High-Density Proximity Mapping Reveals the Subcellular
660 Organization of mRNA-Associated Granules and Bodies. Molecular Cell **69**:517–532.e11.

661 42. **Yue Y**, **Liu J**, **Cui X**, **Cao J**, **Luo G**, **Zhang Z**, **Cheng T**, **Gao M**, **Shu X**, **Ma H**, **Wang**
662 **F**, **Wang X**, **Shen B**, **Wang Y**, **Feng X**, **He C**, **Liu J**. 2018. VIRMA mediates preferential
663 m(6)A mRNA methylation in 3'UTR and near stop codon and associates with alternative
664 polyadenylation. Cell Discov **4**:10.

665 **SUPPLEMENTARY INFORMATION**

666

667 **SUPPLEMENTARY METHODS**

668 **Plasmids**

669 To generate the pPCBP1(N)FLAG-puro plasmid, the complete PCBP1 coding sequence was
670 amplified using PCBP1noAUG-KpnI-FW (5'-AAG CTG GCG GTA CCG GAG ATG CCG
671 GTG TGA CTG-3') and PCBP1-XhoI-RV (5'-TTT TTC TC GAG CTA GCT GCA CCC CAT
672 GCC CTT -3') and the high-fidelity Hot Start Q5 DNA polymerase (NEB). The PCR product
673 was digested with KpnI and XhoI and ligated in a pcDNA3.1(+)-derived plasmid that contained
674 a 3xFLAG tag located downstream of a human cytomegalovirus (CMV) immediate early
675 enhancer/promoter and upstream of a bovine growth hormone (bGH) polyadenylation signal; this
676 insertion left the PCBP1 coding sequence in frame with the upstream 3x FLAG tag. To note, this
677 pcDNA3.1(+)-derived vector also contained a puromycin resistance gene located downstream of
678 a phosphoglycerate kinase 1 (PGK) promoter, and upstream of a simian virus 40 (SV40)
679 polyadenylation signal.

680 To generate the pFLuc-puro plasmid, the complete Firefly luciferase coding sequence
681 was amplified using FLuc-NheI-FW (5'-ATC CGC TAG CAT GGA TTA CAA GGA C-3') and
682 FLuc-XhoI-RV (5'-AAG GTA TCT CGA GTT AGT AAA CAA GAT AAT TGC TCC TAA
683 AGT A-3') using the high-fidelity Hot Start Q5 DNA polymerase (NEB). The PCR product was
684 digested with NheI and XhoI and ligated into the same pcDNA3.1(+)-derived plasmid, between
685 the CMV enhancer/promoter and the bGH polyadenylation signal; this insertion removed the
686 3xFLAG tag.

687 The pJ6/JFH1 FL RLuc WT ("RLuc-wt") viral sequence contains include a *Renilla* luciferase
688 (RLuc) reporter gene inserted between p7 and NS2 (1). The pJ6/JFH-1 FL RLuc-NS5A-GFP
689 ("NS5A-GFP") plasmid contains a GFP insertion between P2390 and L2391 within the NS5A
690 domain III, as previously described (2). The NS5A-GFP region was subcloned into the pJ6/JFH-
691 1 FL RLuc WT backbone using the *AvrII* and *XbaI* restriction sites.
692 To construct a JFH-$1_T$-RLuc viral genome template, a MluI site was created between the
693 p7 and NS2 genes by PCR amplification of the pJFH-$1_T$ plasmid using JFH1-p7NS2-MluI-FW
694 (5'-CCT ATG ACG CGT CTG TGC ACG GAC AGA TAG GC-3'), JFH1-p7NS2-MluI-RV (5'-
695 CAG ACG CGT CAT AGG CAT AAG CCT GCC G-3'), and the high-fidelity Hot Start Q5
696 DNA polymerase (NEB). The PCR product was digested with MluI and dephosphorylated with
697 calf intestinal phosphatase (Quick CIP, NEB) and ligated with an insert containing a *Renilla*
698 luciferase (RLuc) with a C-terminal foot-and-mouth disease virus 2A peptide (FMDV2A), which
699 had been cut out of the pJ6/JFH WT RLuc plasmid by MluI digestion. The correct orientation of
700 the insert was screened by digestion with BstBI and NotI and by sequencing. Once a plasmid
701 with the correct insert orientation was identified, the E1 through NS2 region was cut out using
702 the BsiWI and NotI unique cut sites and ligated into the original pJFH-$1_T$ plasmid backbone. The
703 inserted E1 through NS2 region was sequenced to verify that the PCR amplifications had not
704 introduced any unexpected substitutions.

705

706 **Puromycin selection of cells and infection with JFH-$1_T$**

707 To select cells that would stably express PCBP1(N)FLAG or the FLuc control protein, 15-cm
708 dishes were seeded with 2 x $10^6$ Huh-7.5 cells one day prior to transfection with 36 µg of
709 pPCBP1(N)FLAG-puro or pFLuc-puro plasmid and 30 µL Lipofectamine 2000 diluted in 12 mL

710 Opti-MEM serum-free media (Thermo Fisher Scientific). Two days post-transfection, the media
711 on all transfected plates and one non-transfected plate was changed for complete Huh-7.5 media
712 supplemented with 3 µg/mL puromycin (Thermo Fisher Scientific), which was replenished every
713 two to three days, passaging the cells as necessary. Once all cells in the non-transfected plate
714 were completely dead (within 7 days of selection), selected cells could be used for infection
715 experiments. Selected cells were transfected with siRNA duplexes and infected with JFH-$1_T$ at
716 an MOI of 0.05 as described in the article's main methods; the selection pressure of 3 µg/mL
717 puromycin was maintained in these cells' media until their infection with JFH-$1_T$, after which
718 they were kept in puromycin-free media.

719

720 **REFERENCES**


721 1. **Pietschmann T**, **Kaul A**, **Koutsoudakis G**, **Shavinskaya A**, **Kallis S**, **Steinmann E**, **Abid**
722 **K**, **Negro F**, **Dreux M**, **Cosset F-L**, **Bartenschlager R**. 2006. Construction and
723 characterization of infectious intragenotypic and intergenotypic hepatitis C virus chimeras.
724 PNAS **103**:7408–7413.
725
726 2. **Moradpour D**, **Evans MJ**, **Gosert R**, **Yuan Z**, **Blum HE**, **Goff SP**, **Lindenbach BD**, **Rice**
727 **CM**. 2004. Insertion of green fluorescent protein into nonstructural protein 5A allows direct
728 visualization of functional hepatitis C virus replication complexes. Journal of Virology
729 **78**:7400–7409.
730

731 **SUPPLEMENTARY FIGURES**

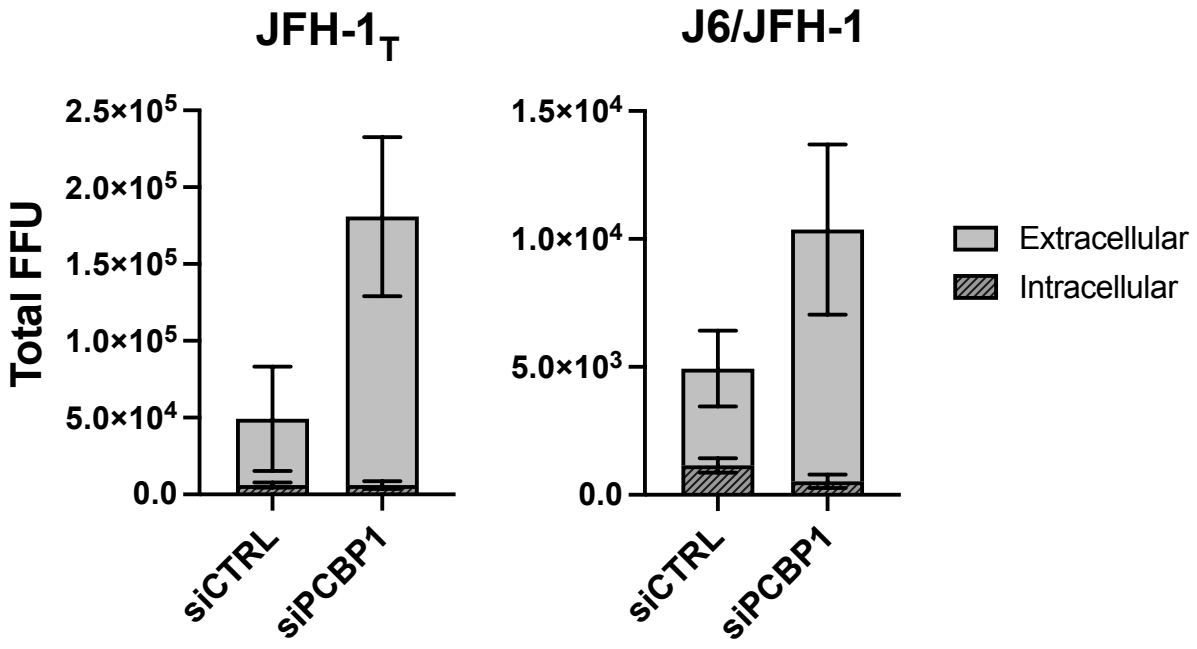


732 **Supplementary Figure S1. PCBP1 knockdown increases the total quantity of infectious**
733 **virions produced by the JFH-1$_T$ and J6/JFH-1 strains.** To calculate the total quantity of
734 infectious virions (FFU) present in a sample, the viral titer (FFU/mL) was multiplied by the total
735 volume of the sample (mL). These data were derived from the same experiments presented in
736 Figure 1 and are representative of three independent biological replicates. Error bars represent
737 the standard deviation of the mean.

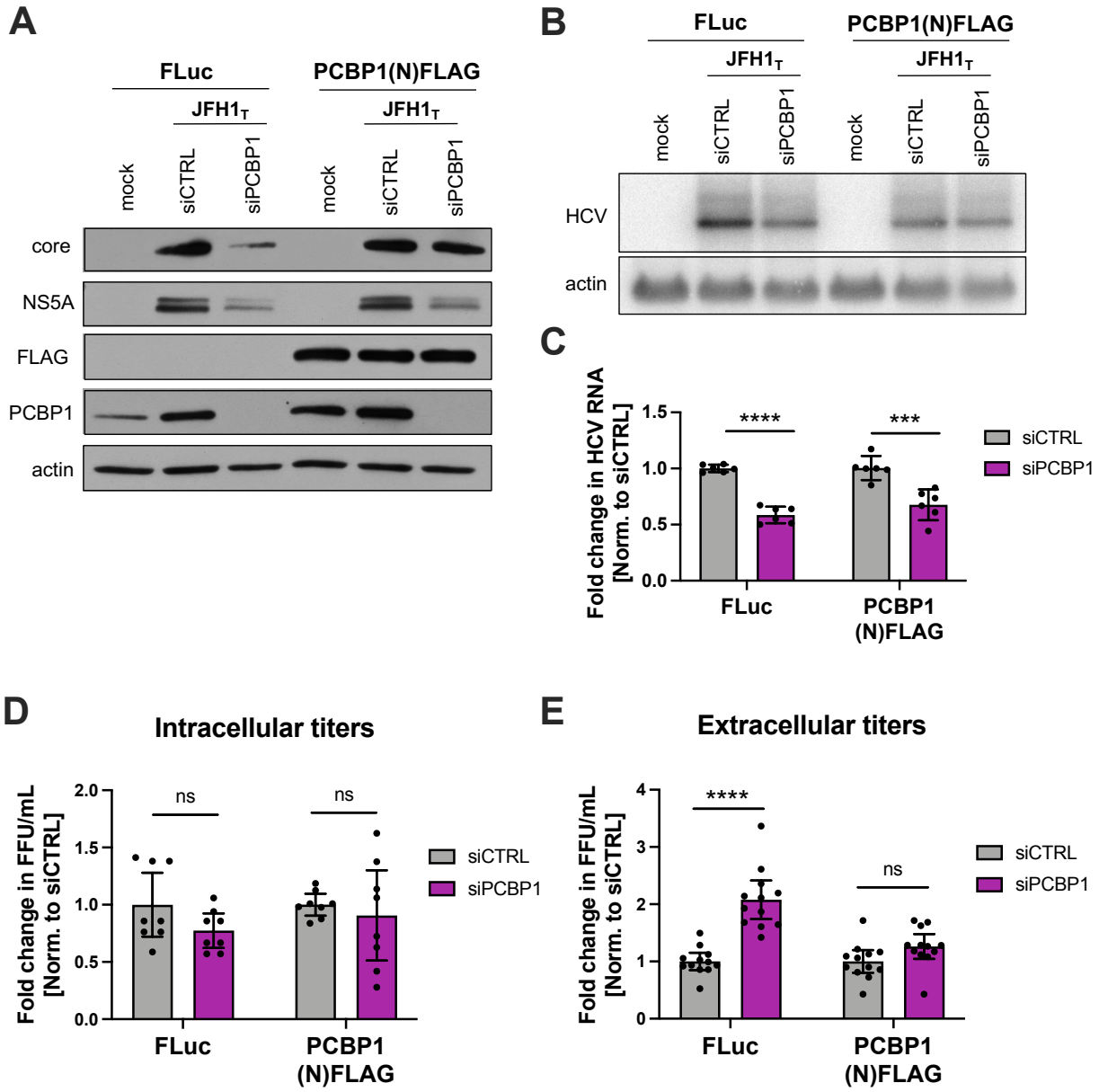


738 **Supplementary Figure S2. Ectopic PCBP1 expression can reduce the impact of endogenous**
739 **PCBP1 knockdown on extracellular viral titers.** Huh-7.5 cells that were puromycin-selected
740 to stably express ectopic Firefly luciferase (FLuc, control) or PCBP1 with a N-terminal FLAG
741 tag (PCBP1(N)FLAG) were transfected with siCTRL or siPCBP1 two days prior to infection
742 with JFH-$1_T$ (MOI 0.05). Three days post-infection, total intracellular protein, RNA, and
743 intracellular and extracellular virus were collected. **(A)** Viral protein expression analysis by
744 Western blot. **(B)** Viral RNA accumulation analysis by Northern blot and **(C)** quantification by

745 RT-qPCR. **(D)** Intracellular and **(E)** extracellular (secreted) virus titers, quantified by FFU assay.
746 For (C-E), data from each experiment was normalized to the mean of the cell-matched siCTRL
747 condition before replicate data were combined. All data are representative of three independent
748 biological replicates, with the exception of (B) which is an N = 1. Error bars represent the
749 standard deviation of the mean. Statistical significance was calculated by paired t-test (ns, not
750 significant; *** $p < 0.001$; **** $p < 0.0001$).
751

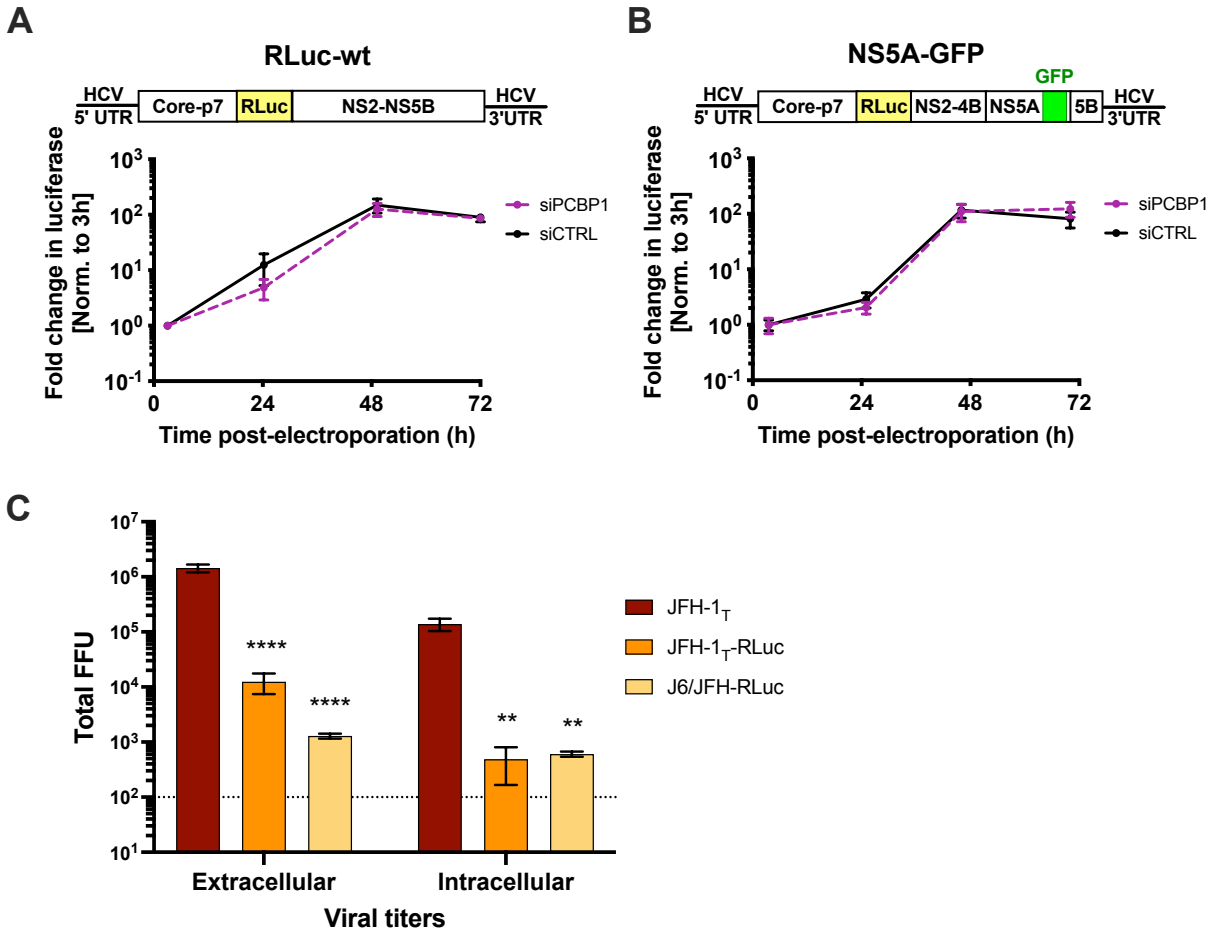


752

753 **Supplementary Figure S3. PCBP1 has no effect on RNA replication in the absence of**
754 **efficient virion assembly, and the addition of a RLuc gene reduces the assembly efficiency**
755 **of HCV genomes.** SiRNA-transfected Huh-7.5 cells were electroporated with 5 µg of (**A**) full-
756 length J6/JFH RLuc WT RNA, or of (**B**) a full-length J6/JFH RLuc with a GFP insertion in the
757 NS5A gene (NS5A-GFP), which had previously been shown to impair virion assembly without
758 impairing viral RNA replication. Luciferase activity was monitored for three days post-
759 electroporation, and RLuc values were normalized to the early timepoint (3h) to control for
760 disparities in electroporation efficiency between experiments. (**C**) Equal amounts (10 µg) of
761 JFH-$1_T$, JFH-$1_T$-RLuc, or J6/JFH-RLuc RNAs were electroporated into Huh-7.5 cells;
762 intracellular and extracellular viruses were collected three days post-electroporation and titered
763 by focus-forming unit assay. Compared with the untagged JFH-$1_T$ RNA electroporations, the
764 extracellular titers were reduced by over 100-fold and 1000-fold for JFH$1_T$-RLuc and J6/JFH-

765 RLuc, respectively; intracellular titers were reduced by more than 200-fold for both luciferase
766 reporter genomes. Data in (A) and (B) are representative of three independent biological
767 replicates; data in (C) is representative of two independent biological replicates, and the limit of
768 detection is indicated. Error bars represent the standard deviation of the mean. Statistical
769 significance was calculated by t-test (** $p < 0.005$, **** $p < 0.0001$)
770